

The 'Dirac' form factor F_1 is the coefficient of γ_μ . Since

$$j_{A\mu}^P = e\gamma_\mu, \quad (\text{A9})$$

and taking

$$j_{V\mu}^P = g_V\gamma_\mu, \quad (\text{A10})$$

$$F_1(p^2) = e + \frac{p^2 X_V g_V}{p^2 + M_V^2}, \quad (\text{A11})$$

which is just the Clementel-Villi form obtained from subtracted dispersion relations.²⁵

In this two-field theory, perturbation calculations could alternatively have been developed in terms of the diagonalized fields ψ_i , defined in Eq. (3.21). This has the advantage that the propagator matrix is diagonal. However, all the complication is transferred to the interaction. The mixing parameters X_i now appear in the currents \mathcal{J}_i and the extraction of the finite parts of the mass operator is considerably less transparent.

²⁵ E. Clementel and C. Villi, *Nuovo Cimento* **4**, 1207 (1956).

Photoproduction of π^+ Mesons from Hydrogen*

M. J. BAZIN† AND J. PINE‡

High Energy Physics Laboratory, Stanford University, Stanford, California

(Received 22 May 1963)

The differential cross section for π^+ photoproduction has been determined at 19 points, at center-of-mass angles from 30 to 150 deg, and at photon energies from 162 to 225 MeV. The data are concentrated near 180 MeV, where a full angular distribution has been determined. The relative values of the cross sections are accurate to 5% or better, and the absolute normalization is accurate to 4%. The experiment provides data of improved accuracy which are in general consistent with previous results. The extrapolation to threshold gives a value for $(k^*/p^*)(d\sigma/d\Omega)^*$ at threshold of $16.1 \pm 0.7 \mu\text{b/sr}$, where k^* , p^* , and $(d\sigma/d\Omega)^*$ are the photon energy, pion momentum, and differential cross section, all in the center-of-mass system.

INTRODUCTION

THE process $\gamma + p \rightarrow \pi^+ + n$ has been studied for a long time, and the reaction provides, particularly at low energy, one of the simplest testing grounds for our knowledge of pion physics. The advent of dispersion theory has resulted in new theoretical calculations,^{1,2} with the most recent ones including the effect of the π - π interaction.^{3,4} The measurements reported here were undertaken to determine differential cross sections with improved accuracy, in the region moderately close to threshold.

The pions were detected with a magnet spectrometer and counter telescope, and the arrangement was appropriate to pions with laboratory momenta from about 55 to 102 MeV/c, at laboratory angles between about 30° and 130°. A complete angular distribution could be measured for a laboratory gamma-ray energy of 180 MeV, while at other energies cross sections were

determined for angles where the pion momentum lay within the experimental range.

When these measurements were begun, the work of Beneventano *et al.*^{5,6} constituted the most accurate and comprehensive study in this energy interval. More recently, Adamovich *et al.*⁷ have performed an experiment using emulsion techniques, with accuracy comparable to this one.

APPARATUS

The intensity of the electron beam of the Stanford Mark III linear accelerator was measured with a secondary emission monitor (SEM)⁸ consisting of three foils of 0.0003-in. aluminum, enclosed in a separate vacuum chamber with 0.003-in. dural windows. The SEM was automatically oscillated both horizontally and vertically in order to average over a foil area about 1.5-in. square. This monitor was calibrated at regular intervals against a Faraday cup of efficiency

* Supported by the U. S. Atomic Energy Commission, Office of Naval Research, and Air Force Office of Scientific Research.

† Present address: Laboratoire de l'Ecole Polytechnique, Paris, France.

‡ Present address: Physics Dept., California Institute of Technology.

¹ G. Chew, M. Goldberger, F. Low, and Y. Nambu, *Phys. Rev.* **106**, 1345 (1957); hereafter referred to as CGLN.

² C. Robinson, University of Illinois, Technical Report No. 8, 1959 (unpublished).

³ J. Ball, *Phys. Rev.* **124**, 2014 (1961).

⁴ J. M. McKinley, Technical Report No. 38, Physics Department, University of Illinois, Urbana, 1962, (unpublished).

⁵ M. Beneventano, C. Bernardini, D. Carlson-Lee, G. Stoppini, and L. Tau, *Nuovo Cimento* **4**, 323 (1956).

⁶ E. L. Goldwasser, in *Proceedings of the 1960 International Conference on High-Energy Physics at Rochester* (Interscience Publishers, Inc., New York, 1960), p. 26.

⁷ M. I. Adamovich, E. G. Gorzhevskaya, V. G. Larionova, N. M. Panova, S. P. Kharlamov, and F. R. Yagudina, in *Proceedings of the 1962 International Conference on High-Energy Physics, CERN*, (CERN, Geneva, 1962).

⁸ G. W. Tautfest and H. R. Fechter, *Rev. Sci. Instr.* **26**, 229 (1955).

(100.0 ± 0.2)%.⁹ In view of the reproducibility of the SEM calibrations, and the performance of the electronic integrators which were used, the beam monitoring uncertainty was about $\pm 0.3\%$. (Uncertainties throughout this paper are estimated standard deviations.)

After traversing the SEM, the electron beam passed through a copper radiator 0.129-radiation length thick. The bremsstrahlung from the radiator, as well as the electron beam, then struck a polyethylene target 0.255-g/cm² thick. The distance from radiator to target was only $4\frac{1}{4}$ in. resulting in a beam diameter at the target of about $\frac{3}{16}$ in. The passage of the electrons through the target gave rise to pions from direct electroproduction which constituted less than 8% of the measured yield.

The polyethylene target was in the form of a rotating wheel, in order to keep its temperature well below the softening point, and the contribution of the carbon was subtracted out by means of measurements with a carbon target 0.299-g/cm² thick. This thickness was chosen to match the pion-ionization losses in the two targets, which were of considerable importance at the lowest energies. In order to keep the carbon subtraction relatively small, the energy of the incident beam, and hence the peak bremsstrahlung energy, was set at 1.16 times the photon energy of interest.

The pions were momentum-analyzed in the double focusing "zero-dispersion" spectrometer which has been described by Alvarez *et al.*¹⁰ The particles were bent through 220-deg by two 110-deg magnets, with the momentum acceptance defined by a slit following the first magnet. The particles were refocused by the second magnet to an achromatic image of the target, with unity magnification. The spectrometer solid angle was about 3.5×10^{-3} sr, limited by the size of the vacuum chamber and the extent of the magnetic fields. For pion momenta below 80 MeV/c, the momentum spread was set at 3.54%, while for momenta from 80 to 102 MeV/c, the spread was 1.80%. The spectrometer field was set with a precision of $\pm 0.1\%$ by means of a rotating coil fluxmeter, and an absolute momentum calibration accurate to $\pm 0.2\%$ was made by using a Cm²⁴⁴ α -particle source. The same source was used to determine the solid angle and momentum acceptance, as described below.

The scintillation counter telescope, shown in Fig. 1, was placed at the spectrometer focus, in a counter house shielded by an average of about 4 ft of iron and lined with lead and borax-loaded paraffin. Pions were selected by requiring counters 1, 2, 3 in coincidence, with 4 in anticoincidence. The thickness of absorber was set to stop pions in the center of counter 3. The anticoincidence counter then eliminated both muons and positrons. Counters 1 and 2 were only $\frac{1}{16}$ -in. thick

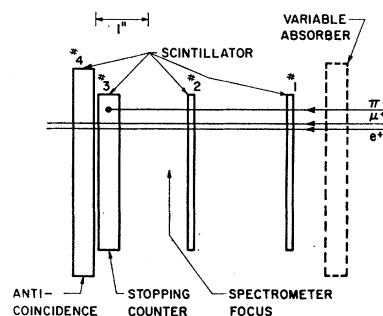


FIG. 1. The scintillation counter telescope.

to provide a threefold coincidence even for very low-energy pions, and to discriminate against positrons by dE/dx . This arrangement reduced background arising from neutron penetration of the shielding to a very low level, and the over-all efficiency for counting positrons was $< 10^{-5}$.

The scintillators were viewed by RCA 6810A photomultipliers whose outputs were fed to transistor discriminators. Pulses exceeding the discrimination level produced outputs of fixed height and for the coincidence counters of length 10 nsec. The coincidence was formed by linearly adding the 1, 2, and 3 discriminator outputs and viewing the sum with a suitably biased discriminator. The output of this discriminator was vetoed by the presence of a pulse from discriminator 4.

The output of the discriminator of the anticoincidence counter was not clipped and had an average length of 45 nsec, with no dead time. Discriminators 1, 2, and 3 had a dead time of, at most, 50 nsec. The only significant correction arising from electronics dead times was due to the high anticoincidence rates at forward angles and low momenta, where there were high positron intensities. This correction was limited to $\leq 4\%$ by carefully maintaining the length of the beam pulse $\geq 0.6 \mu\text{sec}$, and by reducing the beam current when necessary.

Many precautions were taken in order to assure an efficiency of close to 100% for counting pions. During the data taking, pulse-height distributions for all counters were simultaneously recorded, to check that all counts were well above the bias levels. Typically, the biases of counters 1, 2, and 3 were 0.5 V and the most probable pion pulse height was 1.5 V. Counter 4 was biased to detect minimum ionizing particles. As an added check, the coincidence-anticoincidence electronics was duplicated and both sets were run in parallel with slightly different adjustments. While marginal pulses from any counter, or marginal timings, would cause sizable disagreements, the discrepancies observed during the experiment never exceeded one count per 900 pions.

For each pion momentum a "range curve" was taken by varying the absorber thickness in front of the telescope. In this way, the optimum absorber thickness

⁹ D. Yount and J. Pine, Phys. Rev. **128**, 1842 (1962).

¹⁰ R. Alvarez, K. Brown, W. Panofsky, and C. Rockhold, Rev. Sci. Instr. **31**, 556 (1960).

was determined and it was verified that counter 3 was thick enough to contain all the pions and their decay muons.

The fraction of pions scattered out of the telescope was checked for the worst case (highest momentum, and thickest absorber) by measuring the rates as the distance between the absorber and counter 1 was increased. The loss for normal operating geometry was found to be $<1\%$, consistent with calculated estimates.

The data were recorded at intervals over a period of more than a year. The pion yield from polyethylene at one particular setting of the kinematics was measured at least once in each group of runs, to a statistical accuracy of $\pm 3\%$ or better. No variations in this yield, beyond normal statistical fluctuations, were observed.

DATA, CORRECTIONS, UNCERTAINTIES

The π^+ yield, per incident electron, per target proton per cm^2 , may be written as

$$Y = \int \left(\frac{d\sigma}{d\Omega} \right)^* \left(\frac{d\Omega^*}{d\Omega} \right) (\Delta\Omega) P P' N_k dk, \quad (1)$$

where the quantities in the integrand are: $(d\sigma/d\Omega)^*$, the center-of-mass photoproduction cross section; $(d\Omega^*/d\Omega)$, the solid-angle transformation from center of mass to the laboratory; $(\Delta\Omega)$, the spectrometer solid angle; P , the pion survival probability along the path from target to counter telescope; P' , the pion survival probability within the telescope; and $N_k dk$, the number of gamma rays per electron with energy between k and $k+dk$ in the laboratory (including equivalent gamma rays of electroproduction).

Since $(\Delta\Omega)$ is nonzero for only a limited range of pion momenta, and therefore of photon energies, the above equation may be rewritten as

$$Y = \left(\frac{d\sigma}{d\Omega} \right)^* \left(\frac{d\Omega^*}{d\Omega} \right) P P' N_k \frac{dk}{dp} \frac{p}{k} \int (\Delta\Omega) \frac{dp}{p}, \quad (2)$$

where p is the pion laboratory momentum corresponding (via two-body kinematics) to photon energy k . Quantities outside the integral are evaluated at the mean value of k with negligible error. The remaining integral we shall call the spectrometer acceptance.

For fixed setting of the spectrometer momentum slit, with the spectrometer operating far below saturation, the acceptance is a constant, independent of magnet excitation. In this experiment the spectrometer, designed for 300 MeV/c, was used between 55 and 102 MeV/c, and variation of the acceptance was assumed negligible over this range of momenta. For the highest momenta, the slit width was narrowed to assure that all pions stopped within a range interval considerably smaller than the thickness of counter 3. The acceptance under this condition was related to the standard ac-

ceptance by direct intercalibration, with 80-MeV/c pions.

For the determination of relative cross sections, an absolute determination of the acceptance is not necessary. However, to obtain absolute cross sections the acceptance was measured with the help of a thin Cm^{244} α -particle source. The α -particle energy was 5.80 MeV, and the linewidth (arising from back scattering in the source substrate) was about 0.4% . The line shape verified the lack of significant source thickness, exhibiting a sharp edge on the high-energy side with the intensity changing from zero to maximum for an energy change of $<0.1\%$. The source was masked to a size of $\frac{1}{8}$ in. \times $\frac{1}{8}$ in. and placed at the target position, while the pion telescope was replaced by a scintillation counter utilizing a thin sodium-iodide crystal (kindly loaned by F. Bulos). The spectrometer vacuum enclosed both source and counter.

In a straightforward way the rotating coil fluxmeter output corresponding to a pion momentum of 104.0 MeV/c (5.80-MeV α particles; charge = $2e$) was determined, and the central momentum calibration thus established to $\pm 0.2\%$ accuracy. Then, with the momentum slit set at the standard opening for this experiment, the α -particle counting rate was measured as a function of spectrometer field. For a known source intensity the spectrometer acceptance could be found from $\int R dp/p$, with R the α -particle counting rate. The source strength was determined by placing a small collimator in front of the spectrometer, such that the solid angle subtended at the source was known, and such that all particles passing through the collimator would traverse the spectrometer and reach the counter. This procedure also removes the dependence on counter efficiency, although the counter was biased for essentially 100% efficiency.

The acceptance determined as described above was $(1.282 \pm 0.037) \times 10^{-4}$ sr, with the uncertainty being mainly statistical. Owing to pion energy loss by ionization in the target, this acceptance is not correct for determining $(d\sigma/d\Omega)^*$ via Eq. (2). A correction was calculated for each data point, amounting to about 15% in the worst case (lowest pion momentum and longest path in the target). The uncertainty in the correction was negligible. In view of the small target area struck by the beam, the acceptance was expected to remain constant to better than 1% for variations in beam shape and position which could occur. This was verified by measuring the pion rate as a function of beam position.

The survival probabilities P and P' were evaluated using a pion mean life of (25.52 ± 0.30) nsec, obtained by combining the result of Ashkin *et al.*¹¹ with the value

¹¹ J. Ashkin, T. Fazzini, G. Fidicaro, Y. Goldschmidt-Clermont, N. H. Lipman, A. W. Merrison, and H. Paul, *Nuovo Cimento* **16**, 490 (1960).

given by Cohen, Crowe, and Du Mond.¹² The meson path length for the calculation of P was 665 cm, corresponding to the length of the central ray. Owing to the spectrometer optics, all path lengths through the spectrometer are identical except for the effects of second-order aberrations. Between 70 and 90% of the pions decayed before reaching the counters and the uncertainty in P varied from 1.9 to 3.5% over the experimental range of momenta. The probability P' was 0.96, with negligible uncertainty, for all the data.

The gamma-ray intensity, kN_k , was mainly determined from the thick target bremsstrahlung calculations of Alvarez,¹³ of estimated accuracy $\pm 1\%$. The thickness of half the target, as well as of the air and aluminum foils upstream of the target, was included in the radiator thickness. In addition, a photon intensity corresponding to the electroproduction cross section was included in the factor kN_k . This was computed from the theory of Dalitz and Yennie¹⁴ and was at most 8% of the total.

The calculations of Dalitz and Yennie were checked at two representative experimental points by direct measurements of the electroproduction. The results were consistent with the theory, with accuracy $\pm 10\%$. We have assigned an error of $\pm 1\%$ to kN_k to account for the electroproduction uncertainty, which, combined with the estimated error of the bremsstrahlung calculation, gives a final uncertainty of $\pm 1.4\%$.

Of the quantities in Eq. (2) not yet discussed, $(d\Omega^*/d\Omega)$ and $(k/p)(dk/dp)$ are calculated from the photoproduction kinematics, and only the yield Y remains. The raw data from polyethylene and carbon were corrected for the dead time arising from the anticoincidence pulse length, and an uncertainty of half the correction was assigned and combined with the statistical error.

The possibly significant backgrounds were (a) counts arising from neutrons penetrating the shielding, (b) pions from the air around the target, (c) positrons recorded as pions, and (d) muons recorded as pions. Processes (a) and (b) amounted to less than 1% and were experimentally subtracted. From the sharpness of the dependence of counting rate on absorber thickness, the sum of (c) and (d) was estimated at $\lesssim 1\%$. The carbon subtraction automatically accounts for almost all of the background from (c), and no correction for (d) was made. A rough calculation of this background led to an estimate of $< 0.1\%$ in the worst case.

As a further over-all check of backgrounds, pulses from counter 3 were displayed on an oscilloscope triggered by pion counts from the electronics, and

photographed. The $\pi-\mu$ decays were easily observed and the pictures were analyzed as for a π -lifetime measurement. Pictures were obtained at data points for which the pion momenta were 74 and 58 MeV/c, and there was no significant excess of pulses with short (i.e., unresolvable) decay times. The statistical accuracy enabled a limit of 3% to be placed on the total background at each momentum, with the 58-MeV/c data expected to be a "worst case."

Finally, the yield was corrected for pion absorption in the telescope. Stork¹⁵ has directly measured the attenuation of π^+ mesons in carbon in a geometry very similar to that of this experiment. His data are at pion energies from 33 to 68 MeV, the lowest energy corresponding to the highest one for this experiment. By a modest extrapolation of Stork's results, to 20 MeV, the corrections here can be evaluated with satisfactory accuracy. For 102-MeV/c pions the correction is largest and equal to $(2.5 \pm 1.0)\%$. Below 80 MeV/c the correction becomes negligible.

Table I summarizes the experimental results and the uncertainties. The relative errors do not include uncertainties which affect only the over-all normalization. The normalization error is $\pm 4.2\%$ and is dominated by three contributions: $\pm 2.9\%$ from the spectrometer acceptance, $\pm 1.4\%$ from the gamma-ray intensity, and $\pm 2.7\%$ from the pion-decay correction. Owing to the fact that the data were taken at constant

TABLE I. Experimental results. Photon energies k are in the laboratory, and pion angles θ^* are in the center-of-mass system. The pion momentum p_m is the spectrometer setting, which takes account of ionization loss in the target. The relative errors include all uncertainties except those which affect the absolute normalization. The absolute errors are derived by combining the normalization uncertainty of $\pm 4.2\%$ with the relative errors.

k (MeV)	θ^* (deg)	p_m (MeV/c)	$(d\sigma/d\Omega)^*$ ($\mu\text{b/sr}$)	Absolute error (%)	Relative error (%)
162	70	54.7	5.16	± 6.6	± 5.1
165	90	54.6	5.81	± 6.9	± 5.5
165	67	63.2	5.86	± 6.6	± 5.1
167	90	58.6	6.25	± 6.6	± 5.1
170	65	75.7	6.32	± 6.4	± 4.8
170	90	64.2	6.32	± 7.4	± 6.1
170	110	54.6	6.78	± 6.9	± 5.5
180	35	101.7	6.78	± 6.5	± 5.0
180	60	94.3	6.84	± 5.7	± 3.9
180	90	81.7	7.41	± 7.0	± 5.6
180	105	74.3	7.85	± 5.2	± 3.1
180	130	62.5	8.43	± 6.3	± 4.7
180	140	58.4	8.45	± 5.9	± 4.1
180	150	54.6	7.83	± 6.2	± 4.6
184	58	101.7	6.82	± 5.7	± 3.9
194	90	101.7	8.71	± 5.6	± 3.7
194	120	85.9	9.64	± 6.5	± 5.0
194	150	73.0	9.80	± 6.3	± 4.7
225	150	101.9	12.35	± 5.5	± 3.6

¹² E. Cohen, K. Crowe, and J. DuMond, *The Fundamental Constants of Physics* (Interscience Publishers, Inc., New York, 1957).

¹³ R. A. Alvarez, Stanford University High-Energy Physics Laboratory Report HEPL-228, 1961 (unpublished).

¹⁴ R. Dalitz and D. Yennie, *Phys. Rev.* **105**, 1598 (1957).

¹⁵ D. Stork, *Phys. Rev.* **93**, 868 (1954).

k/E_0 , where E_0 is the incident electron energy, the relative error in the bremsstrahlung intensity is negligible. The contribution from electroproduction varies relatively little over the range of the experiment and, thus, introduces an absolute uncertainty but negligible relative error. The mean value of the uncertainty arising from the π lifetime is treated as a normalization error, while its variation from highest to lowest momentum of the experiment is included in the relative errors.

The absolute uncertainties in Table I are simply the relative errors combined with the normalization error. For any particular cross section, this error applies, while for studies involving a group of cross sections the two types of uncertainty may most usefully be kept separate.

DISCUSSION

Angular Distribution

The results listed in Table I are graphed in Figs. 2 and 3. In Fig. 3, the angular distribution at 180 MeV is compared with the measurements of Beneventano *et al.*⁵ and of Adamovich *et al.*⁷ The data of Beneventano are corrected by +10%, as indicated by Goldwasser,⁶ and points at both 180 and 185 MeV have been combined, using the energy dependence given by Robinson's calculations² to convert the 185-MeV data to 180 MeV. The theory has similarly been used to translate the data of Adamovich *et al.* from 185 to 180 MeV. The change in the cross sections is at most 7% (at backward angles), and, in view of the fit between experiment and calculations shown in Fig. 2, the error introduced by this process should be small. The consistency between experiments is seen to be excellent. At other photon energies, the agreement between this experiment and that of Adamovich *et al.* remains good.

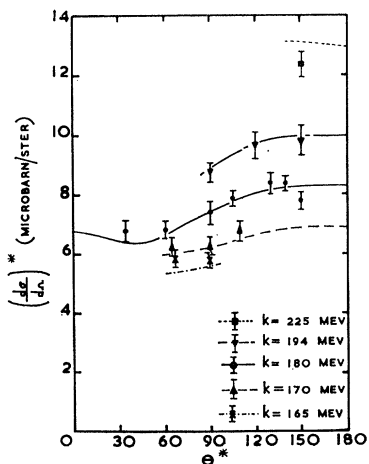


FIG. 2. The measured photoproduction cross sections, shown with relative errors only. The absolute normalization is uncertain by $\pm 4.2\%$. The curves are from the dispersion theory calculation of Robinson.

The calculations of Robinson, shown in Figs. 2 and 3 use the one-dimensional dispersion relations of Chew *et al.*¹ (CGLN), with the S -wave phase shifts directly from experiment and the small P -wave phase shifts from effective-range formulas. Terms proportional to $(m_\pi/m_p)^2$ are neglected, and the over-all accuracy is estimated at $\pm(5-10)\%$. The consistency between theory and experiment appears to be excellent.

Ball's calculation,³ shown in Fig. 3, uses the Mandelstam representation and is fully relativistic. However, all the small P -wave phase shifts have been set equal to zero. The theory is aimed at describing the cross sections near threshold, with an estimated accuracy of 5%.¹⁶ At backward angles at 180 MeV, the two calculations differ by about 10%, and the fit of the Robinson calculation appears superior. At 200 MeV, the difference becomes 21% at backward angles, and the Ball theory is clearly inconsistent with the data at this higher energy.

The importance of the small P -wave shifts in Robinson's calculation was checked by changing δ_{11}

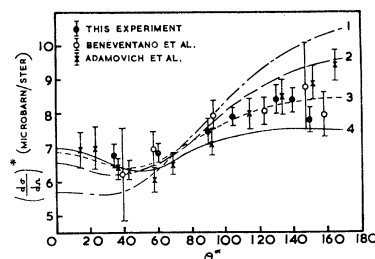


FIG. 3. The angular distribution at 180 MeV from this experiment and others. The data of this experiment are subject to a normalization error of $\pm 4.2\%$ not shown on the graph. Curves 1 and 2 are from McKinley's calculation, with phase shift sets "Y" and "X," respectively; curve 3 is from Robinson's calculation; and curve 4 is from Ball's calculation.

from -2.5° , as given by the effective range formula, to -1.25° . The angular distribution was changed by $+8\%$ at backward angles and -10% at forward angles. Similarly, large effects resulted from individually changing the other small P -wave phase shifts by one or two degrees. The photoproduction cross sections appear to provide a quite sensitive test for a set of phase shifts, without enabling one to define individual phases.

McKinley⁴ has recently reexamined the calculation of photoproduction amplitudes by means of CGLN theory. Among other refinements, he has used new polynomial fits to all the phase shifts. Figure 3 shows the McKinley results for two sets of phase shifts which differ in their values for δ_1 , δ_{11} , and δ_{13} . Set X tries to fit all experimental data; set Y ignores three experiments at pion energies of 100–170 MeV, a procedure which leads to simpler polynomials. We have again used the energy dependence of the Robinson

¹⁶ J. Ball (private communication).

theory to convert the calculations from 185 to 180 MeV. Neither set of phase shifts gives satisfactory agreement with experiment.

Energy Dependence

Figures 4 and 5, in which the quantity $|M|^2$, defined by

$$|M|^2 = \frac{k^*}{p^*} \left(\frac{d\sigma}{d\Omega} \right)^*,$$

is shown as a function of k , summarize the measured variation of the cross section with photon energy (starred quantities are evaluated in the center-of-mass system). It has long been considered convenient to examine the energy dependence at $\theta^* = 90^\circ$, where the S - P interference gives no contribution, and Fig. 4 continues this tradition. The calculation of Robinson is seen to be in good agreement with the data, and its energy dependence was used to extrapolate to threshold. The threshold value of $|M|^2$ derived in this way is $|M|_0^2 = (15.9 \pm 0.8) \mu\text{b/sr.}$, where the uncertainty

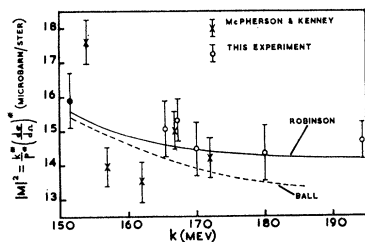


FIG. 4. Threshold extrapolation at 90° c.m. The experimental points are shown with relative errors, but the extrapolated value of $|M|^2$, shown by the solid circle, includes the normalization error. Curves from the calculations of Robinson and Ball are shown, and the extrapolation is based on the energy dependence of the Robinson calculation.

is dominated by the normalization error. The cross sections given by McPherson and Kenney¹⁷ are also shown and their extrapolated value is consistent with this experiment.

Baldin¹⁸ has pointed out that for the kinematical condition $k^*(E^* - p^* \cos\theta^*) = m_\pi k_{\text{threshold}}^*$, which keeps the momentum transfer to the nucleon equal to its threshold value, the dispersion integrals do not involve the unphysical region. Regardless of the importance of this restriction (particularly at low energies), a number of experimental points along the "Baldin line" have been measured. Figure 5 shows the results, including a set of relative measurements, described in the Appendix, which were made with a liquid-hydrogen target and a gamma-ray beam swept free of electrons and positrons. These data are normalized to the solid

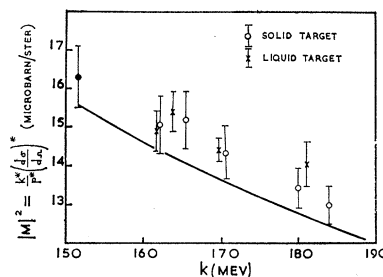


FIG. 5. Threshold extrapolation along the "Baldin line." The experimental points are shown with relative errors, but the extrapolated value of $|M|^2$, shown by the solid circle, includes the normalization error. The theoretical curve from the calculation of Robinson is shown, and the energy dependence of this calculation was used for the extrapolation.

target data and merely constitute a check of the energy dependence.

The Robinson calculation is seen to have the correct shape and to differ by about $(5 \pm 5)\%$ from the absolute data. The extrapolation to threshold, using the shape of the Robinson curve, yields the value $|M|_0^2 = (16.3 \pm 0.8) \mu\text{b/sr.}$ Combining the two extrapolations, the final value for the threshold matrix element is given by

$$|M|_0^2 = (16.1 \pm 0.7) \mu\text{b/sr.}$$

The normalization error dominates, and no contribution for the uncertainty in the shape of the extrapolation curves has been included. This result is consistent with previous estimates.^{7,19,20}

Ball's theory predicts a threshold value $|M|_0^2 = 15.4$ accurate to about 5%, with no π - π interaction.

Rho-Meson Effects

A number of authors have pointed out that the photoproduction cross section may be influenced by the pion-pion interaction in the $T=J=1$ state (the ρ meson).^{3,21,22} The importance of this effect depends on the strength of the γ - π - ρ coupling, which has been characterized by the parameter Λ .

If the experimental data are found to deviate from a theory which ignores ρ -meson effects, the discrepancy may be ascribed either to such effects or to other shortcomings of the theory. With regard to π^+ photoproduction at the energies studied here, the accuracy of the theory is limited by inadequate knowledge of the phase shifts as well as by other difficulties.²³ If McKinley's version of CGLN theory is used, the discrepancy at backward angles shown in Fig. 3 indicates $\Lambda \sim 0.7 \pm 0.7$. The large uncertainty reflects our guess

¹⁹ J. Hamilton and W. Woolcock, Phys. Rev. **118**, 291 (1960).

²⁰ J. Walker, Nuovo Cimento **21**, 577 (1961).

²¹ M. Gourdin, D. Lurié, and A. Martin, Nuovo Cimento **18**, 933 (1960).

²² B. de Tollis, E. Ferrari, and H. Munczek, Nuovo Cimento **18**, 198 (1960).

²³ G. Höhler and K. Dietz, Institut für Theoretische Kernphysik der Technische Hochschule, Karlsruhe, 1963 (unpublished).

¹⁷ D. McPherson and R. Kenney, Bull. Am. Phys. Soc. **6**, 523 (1961).

¹⁸ A. M. Baldin, Zh. Eksperim. i Teor. Fiz. **39**, 1151 (1960) [translation: Soviet Phys.—JETP **12**, 800 (1961)].

as to the reliability of the theory, and cannot be justified in detail. The evaluation of Λ has been done from McKinley's calculation, which uses the "bipion" amplitude of De Tollis and Verganelakis.²⁴ The result is consistent with previous estimates of Λ , which have been summarized in a separate paper describing measurements we have made of the π^-/π^+ ratio for photo-production from deuterium.²⁵

Summarizing the discussion, the measurements reported here provide data of improved accuracy, consistent with other experiments, and at present the interpretation is limited at least as much by theoretical uncertainty as by the experimental errors.

APPENDIX: LIQUID TARGET DATA

During the course of this experiment, measurements of the π^-/π^+ ratio from deuterium were made²⁵ utilizing

²⁴ B. de Tollis and A. Verganelakis, *Nuovo Cimento* **22**, 406 (1961).

²⁵ J. Pine and M. Bazin (to be published).

a liquid target and a beam swept free of electrons. By filling the target with hydrogen, the relative cross sections shown in Fig. 5 were obtained at a fixed laboratory angle of 47 deg. Over the energy range studied, this angle is always within 2° of that defined by Baldin's kinematical condition.

The same spectrometer and counters were used as for the solid target data. However, there was no carbon subtraction, no electroproduction, and a much lower flux of positrons into the spectrometer. In exchange for these advantages, the beam spot at the target was larger and the target itself constituted a rather extended source of pions. As a result, the arrangement lent itself best to the measurement of relative cross sections at a fixed laboratory angle, so that the spectrometer acceptance could safely be assumed to remain constant. The electron energy was also held fixed at 239 MeV, to maintain a constant beam size.

The errors in these data are mainly statistical, and the consistency with the solid target data is seen to be good.

Theorem on the Shrinking of Diffraction Peaks*

ALBERT C. FINN

Institute of Theoretical Physics, Department of Physics, Stanford University, Stanford, California

(Received 5 June 1963)

It is shown that the width of a diffraction peak divided by $\frac{1}{2}\sigma(s, t=0)$ cannot decrease faster at high energies than a constant times $(\ln s)^{-6}$. This follows from unitarity and analyticity in the largest Lehmann ellipse consistent with perturbation theory.

THERE has been considerable interest lately in the behavior of diffraction peaks at high energies. In Fig. 1, we show a typical angular distribution¹ $\sigma(s, t)$

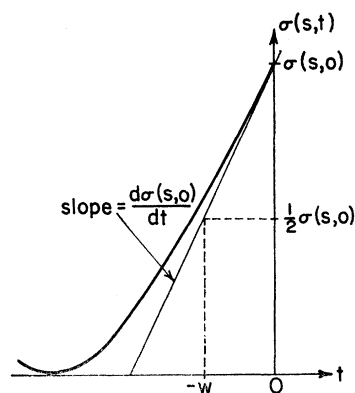


FIG. 1. A typical angular distribution $\sigma(s, t)$ is shown. The width of the diffraction peak w is defined by the equation $w = \sigma(s, 0) / [2d\sigma(s, 0)/dt]$.

plotted versus t the invariant four-momentum transfer. s is the square of the total center-of-mass energy. t is related to the center-of-mass three-momentum q and the scattering angle θ by the relation $t = -2q^2(1 - \cos\theta)$. The physical scattering region is $t \leq 0$. We set $\hbar = c = 1$ and measure all energies in units of the mass of the lightest particle involved in the scattering process. The width of a diffraction peak w is defined by

$$w = \frac{\sigma(s, 0)}{2d\sigma(s, 0)/dt}.$$

We will prove that $d\sigma(s, t)/dt$ (the slope of the angular distribution) is bounded from above by $C(\ln s)^6$, where C is a constant independent of s and t . From this it follows that the width divided by $\frac{1}{2}\sigma(s, 0)$ cannot decrease faster than a constant times $(\ln s)^{-6}$.

In proving this result we will follow the method used by Greenberg and Low² to set bounds on high-energy cross sections from analyticity in Lehmann ellipses.

² O. W. Greenberg and F. E. Low, *Phys. Rev.* **124**, 2047 (1961).

* The study was supported by the U. S. Air Force Office of Scientific Research Grant AF-AFSOR-62-542.

¹ See, for example, several papers in session H2 of the *Proceedings of the 1962 Annual International Conference on High-Energy Physics at CERN* (CERN, Geneva, 1962).